17th International Conference on the Application of Computer
Science and Mathematics in Architecture and Civil Engineering
K. Gürlebeck and C. Könke (eds.)
Weimar, Germany, 12–14 July 2006

# WAVELET ANALYSIS AND FREQUENCY BAND DECOMPOSITIONS

**K. Markwardt**

*Bauhaus-University Weimar, Institute for Mathematics/Physics*
*Weimar, Federal Republic of Germany*
E-mail: klaus.markwardt@bauing.uni-weimar.de

**Keywords:** Time Frequency Analysis, Biorthogonal Wavelets, Wavelet Packages, Frequency Bands, Center of Frequency

**Abstract.** *In many applications such as parameter identification of oscillating systems in civil enginee-ring, speech processing, image processing and others we are interested in the frequency con-tent of a signal locally in time. As a start wavelet analysis provides a time-scale decomposition of signals, but this wavelet transform can be connected with an appropriate time-frequency decomposition. For instance in Matlab are defined pseudo-frequencies of wavelet scales as frequency centers of the corresponding bands. This frequency bands overlap more or less which depends on the choice of the biorthogonal wavelet system. Such a definition of frequency center is possible and useful, because different frequencies predominate at different dyadic scales of a wavelet decomposition or rather at different nodes of a wavelet packet decomposition tree. The goal of this work is to offer better algorithms for characterising frequency band behaviour and for calculating frequency centers of orthogonal and biorthogonal wavelet systems. This will be done with some product formulas in frequency domain. Now the connecting procedu-res are more analytical based, better connected with wavelet theory and more assessable. This procedures doesn't need any time approximation of the wavelet and scaling functions. The method only works in the case of biorthogonal wavelet systems, where scaling functions and wavelets are defined over discrete filters. But this is the practically essential case, because it is connected with fast algorithms (FWT, Mallat Algorithm). At the end corresponding to the wavelet transform some closed formulas of pure oscillations are given. They can generally used to compare the application of different wavelets in the FWT regarding it's frequency behaviour.*

## 1 INTRODUCTION

In many applications such as parameter identification of oscillating systems, speech processing, atrial signal-averaged electrocardiograms and others we are interested in the frequency content of a signal locally in time. Such applications are connected with so called non-stationary signals, where essentiell parameters (frequency, phase etc.) evolve over time. This signals have transitory characteristics like drifts, trends, abrupt changes, beginnings and ends of events. Special cases are chirp signals, which can formulate with the help of harmonic functions. Chirp signals with a linear or quadratic time-frequency pattern are used in [16] to test algorithms in time frequency analysis, which are developed on the basis of wavelet or wavelet packet decompositions.

As a start wavelet analysis provides a time-scale decomposition of signals. How this is connected with an appropriate time-frequency decomposition? In [16] for instance is given the procedure scal2frq(a,'wname',delta), which associates a pseudo-frequency to the scale a for a given wavelet 'wname'. Of course this pseudo-frequency depends on the sampling period delta. So especially one get a pseudo-period or pseudo-frequency for every discrete scale level produced by FWT. FWT is the Fast Wavelet Transform realized by the Mallat-algorithm. It decomposes the signal in a hierarchical set of approximations and details.

The procedure scal2frq needs freq = centfrq('wname',iter), which returns a frequency center of a given wavelet in Hertz. Here the parameter iter is the number of iterations used by the wavefun-algorithm to approximate the wavelet function. On this by 'wavefun' produced time array the algorithm 'centfrq' applies the Fast Fourier-transform. So there is provided a basis for producing the amplitude spectrum of the wavelet. Then there center frequency is simply defined by the argument which maximizes this spectrum. Such procedures are possible because different frequencies predominate at different dyadic scales of a wavelet decomposition or rather at different nodes of a wavelet packet decomposition tree. Every scale or node can be interpreted as a frequency band with a center. Dependent on the choice of the wavelet this frequency bands overlap more or less.

The goal of this work is to offer better algorithms for characterising frequency band behavior and calculating frequency centers of orthogonal and biorthogonal waveletssystems. This will be done with some product formulas in frequency domain, cp.[12], [7]. Now the connecting procedures are more analytical based, better connected with wavelet theory, more assessable and quicker. This procedures doesn't need any time approximation of the wavelet function. So also in practice the necessary link between scale and frequency will be improved. The method only works in the case of orthogonal or biorthogonal Wavelet systems, where scaling functions and wavelets are defined over discrete filters. But this is the practically essential case, because it is connected with fast algorithms (FWT, Mallat algorithm).

## 2 BASICS FROM WAVELET THEORY

Here finite discrete filters are defined as elements of $\mathbb{R}^{\mathbb{Z}}$ with finite many entries different from 0. With appropriate indices $s, u \in \mathbb{Z}$ all used filters are assumed of the type

$$c = \left( \cdots, \ 0, \ 0, \ c_s, \ \cdots, \ c_u, \ 0, \ 0, \ \cdots \right). \tag{1}$$

A biorthogonal wavelet system is connected with four filters $\{h, \tilde{h}, g, \tilde{g}\}$ which satisfy the following properties

$$\sum_k h_k \, \tilde{h}_{k+2l} = \delta_{l0} \,, \qquad \sum_k g_k \, \tilde{g}_{k+2l} = \delta_{l0} \,, \tag{2}$$

$$\sum_k \tilde{h}_k \, g_{k+2l} = 0 \,, \qquad \sum_k h_k \, \tilde{g}_{k+2l} = 0 \,, \tag{3}$$

$$\sum_k h_k = \sum_k \tilde{h}_k = \sqrt{2} \,, \qquad \sum_k g_k = \sum_k \tilde{g}_k = 0 \,. \tag{4}$$

The two integers $s, u$ are chosen such that all four filters can be written in the form (1) with the same minimal $[s, u] \subset \mathbb{Z}$. It follows

$$\sum_k (-1)^k h_k = 0 \quad \text{and} \quad \sum_k (-1)^k \tilde{h}_k = 0. \tag{5}$$

Further conclusions and relations to other biorthogonal filter representations are given in [12], cp. [7], [8], and for the special orthogonal case in [1], [9]. If this filters fulfill some further properties, which are related to the eigenvalues of two Lawton matrices, then by

$$\varphi(t) = \sqrt{2} \sum_k h_k \, \varphi(2t - k) \,, \qquad \psi(t) = \sqrt{2} \sum_k g_k \, \varphi(2t - k) \tag{6}$$

$$\tilde{\varphi}(t) = \sqrt{2} \sum_k \tilde{h}_k \, \tilde{\varphi}(2t - k) \qquad \tilde{\psi}(t) = \sqrt{2} \sum_k \tilde{g}_k \, \tilde{\varphi}(2t - k) \tag{7}$$

$$\int_{-\infty}^{\infty} \varphi(t) \, dt = \int_{-\infty}^{\infty} \tilde{\varphi}(t) \, dt = 1 \,. \tag{8}$$

scaling functions $\varphi, \, \tilde{\varphi} \in L^2(\mathbb{R})$ and wavelets $\psi, \, \tilde{\psi} \in L^2(\mathbb{R})$ are determined uniquely. They have compact support, such that with the above defined $s, \, u$

$$supp(\varphi) \subset [s, u] \,, \qquad supp(\tilde{\varphi}) \subset [s, u] \tag{9}$$

is valid. For $i, j, k, l \in \mathbb{Z}$ the deduced variants

$$\varphi_{j,k}(t) = \sqrt{2^{-j}} \, \varphi(2^{-j} \, t - k), \qquad \psi_{j,k}(t) = \sqrt{2^{-j}} \, \psi(2^{-j} \, t - k), \quad \cdots \,, \quad \cdots \,, \tag{10}$$

satisfy the biorthogonal relations

$$\langle \varphi_{j,k} \, , \, \tilde{\varphi}_{j,l} \rangle = \delta_{k,l} \tag{11}$$

$$\langle \varphi_{i,k} \, , \, \tilde{\psi}_{j,l} \rangle = \langle \tilde{\varphi}_{i,k} \, , \, \psi_{j,l} \rangle = 0 \qquad \text{for} \quad i \geq j \tag{12}$$

$$\langle \psi_{i,k} \, , \, \tilde{\psi}_{j,l} \rangle = \delta_{i,j} \cdot \delta_{k,l} \,. \tag{13}$$

In particular $\{\psi_{i,k}\}$ and $\{\tilde{\psi}_{i,k}\}$ build a pair of biorthogonal Riesz bases in $L^2(\mathbb{R})$, cp.[7] and [8]. Between different function levels filter equations of the type

$$\varphi_{j+1,r} = \sum_{\nu=s+2r}^{u+2r} h_{\nu-2r} \, \varphi_{j,\nu} \;\; , \qquad \psi_{j+1,r} = \sum_{\nu=s+2r}^{u+2r} g_{\nu-2r} \, \varphi_{j,\nu} \tag{14}$$

and

$$\tilde{\varphi}_{j+1,r} = \sum_{\nu=s+2r}^{u+2r} \tilde{h}_{\nu-2r}\, \tilde{\varphi}_{j,\nu}\,, \qquad \tilde{\psi}_{j+1,r} = \sum_{\nu=s+2r}^{u+2r} \tilde{g}_{\nu-2r}\, \tilde{\varphi}_{j,\nu}\,. \tag{15}$$

are valid. Using here $\tilde{\varphi},\ \tilde{\psi}$ as analysis functions and $\varphi,\ \psi$ as synthesis functions we get for the projection on the level $J$

$$(\mathbf{P}_J f)(t) = \sum_k \tilde{S}_{Jk}\, \varphi_{J,k}(t) \qquad with \qquad \tilde{S}_{Jk} = \langle f\ ,\ \tilde{\varphi}_{J,k} \rangle\ . \tag{16}$$

Let $f_s$ be a sampled signal. After suitable dilation it can be approximated by (16) on the level $J = 0$ using wavelet sampling approximation or an preprocessing method for getting the basic coefficients $\tilde{S}_{0k}$, cp.[12].

$$P_0(f)(t) = \sum_k \tilde{S}_{0,k}\, \varphi_{0,k}(t) \tag{17}$$

FWT results from successive applying of the decomposition formulas

$$\tilde{S}_{l+1,k}\ = \sum_r \tilde{h}_{r-2k}\, \tilde{S}_{l,r}\,, \qquad \tilde{W}_{l+1,k}\ = \left\langle f\ ,\ \tilde{\psi}_{l+1,k} \right\rangle = \sum_r \tilde{g}_{r-2k}\, \tilde{S}_{l,r}. \tag{18}$$

It gives the corresponding representation to (17) with the wavelet coefficients $\tilde{W}_{lk}$ of different levels $l$ and the scaling coefficients $\tilde{S}_{Lk}$ of the level $L$

$$(\mathbf{P}_0 f)(t) = \sum_k \tilde{S}_{Lk}\, \tilde{\varphi}_{L,k}\ + \sum_{l=1}^{L} \left\{ \sum_k \tilde{W}_{lk}\, \psi_{l,k} \right\}. \tag{19}$$

With increasing $l$ the frequency center of the inner sums

$$(\mathbf{Q}_l f)(t) = \sum_k \tilde{W}_{lk}\, \psi_{l,k} \tag{20}$$

decreases step by step by the factor $0.5$. Here every wavelet $\psi_{l,k}$ has the same amplitude spectrum.

Using wavelet packets induced by appropriate $\{h, \tilde{h}, g, \tilde{g}\}$ you get trees with the possibility of stronger locally frequency resolution, cp.[3], [18].
The inverse formula of (18) is known as

$$\tilde{S}_{l,k}\ = \sum_r h_{k-2r}\, \tilde{S}_{l-1,r}\ + \sum_r g_{k-2r}\, \tilde{W}_{l-1,r}\,. \tag{21}$$

## 3 FREQUENCY BAND DECOMPOSITIONS

With the Fourier-transform

$$\hat{f}\,(\xi) := \int_{-\infty}^{\infty} f\,(t)\, e^{-i\,2\,\pi\,\xi t}\, dt \tag{22}$$

and the so called Fourier-filters

$$m_o(\xi) = \frac{\sqrt{2}}{2} \sum_k h_k\, e^{-i2k\pi\xi}, \qquad m_1(\xi) = \frac{\sqrt{2}}{2} \sum_k g_k\, e^{-i2k\pi\xi} \tag{23}$$

in frequency domain the scaling equations (6) become the size

$$\hat{\varphi}(\xi) = m_o\left(\frac{\xi}{2}\right)\,\hat{\varphi}\left(\frac{\xi}{2}\right) \qquad \text{and} \qquad \hat{\psi}(\xi) = m_1\left(\frac{\xi}{2}\right)\,\hat{\varphi}\left(\frac{\xi}{2}\right). \tag{24}$$

This are the corresponding frequency representations of the defining scaling equations (6). The left equation in (24) yields to a formula for the Fourier-transform of the scaling function $\varphi$

$$\hat{\varphi}(\xi) = \prod_{j=1}^{\infty} m_o\left(2^{-j}\xi\right), \tag{25}$$

if the requirements of Lemma 3.1 in [7] are fulfilled, cp. [12]. In the case of mostly used wavelets, for instance those which are implemented in the Wavelet-Toolbox of Matlab, cp.([16]), 10 factors of the product (25) are enough to get a very good approximation of $\hat{\varphi}$ in the normed interval $[0, 1]$. This gives the possibility to improve considerably the wavelet procedures in ([16]), which are used for determining pseudofrequency centers for wavelet bands. Beyond it the frequency bands of wavelet scales and the frequency overlapping of neighbored scales can be sharper characterized. So time-frequency-analysis becomes more exactly. In many applications one can now better decide the question which wavelet systems are to choose.

Now further formulas will be derived and some tables will be established to realize the above formulated goals. This formulas give also the possibility of a good visualization of the corresponding coherences.

With the sequence of substitutions

$$t \quad \longmapsto \quad t-k \quad \longmapsto \quad 2^{-j}\,t-k$$

and using standard formulas for Fourier-transform one get for (10) the equations

$$\hat{\varphi}_{j,k}(\xi) \;=\; \sqrt{2^j}\,exp(-i\cdot 2^{j+1}k\,\pi\,\xi)\cdot\hat{\varphi}(2^j\,\xi) \tag{26}$$

$$\hat{\psi}_{j,k}(\xi) \;=\; \sqrt{2^j}\,exp(-i\cdot 2^{j+1}k\,\pi\,\xi)\cdot\hat{\psi}(2^j\,\xi). \tag{27}$$

Now by

$$\hat{\varphi}(2\,\xi) = m_o(\xi)\,\hat{\varphi}(\xi), \qquad \hat{\psi}(2\,\xi) = m_1(\xi)\,\hat{\varphi}(\xi) \tag{28}$$

and

$$\hat{\varphi}(2^L\,\xi) = \hat{\varphi}(\xi)\prod_{j=0}^{L-1} m_0(2^j\xi), \qquad \hat{\psi}(2^L\,\xi) = \hat{\varphi}(\xi)\,m_1(2^{L-1}\xi)\prod_{j=0}^{L-2} m_0(2^j\xi) \tag{29}$$

frequency representations of the dilation-translation variants (10) can be deduced

$$\hat{\psi}_{1,k}(\xi) \;=\; \hat{\varphi}(\xi)\,\cdot exp(-i\cdot 4k\pi\xi)\cdot\sqrt{2}\,m_1(\xi) \tag{30}$$

$$\hat{\psi}_{2,k}(\xi) \;=\; \hat{\varphi}(\xi)\,\cdot exp(-i\cdot 8k\pi\xi)\cdot 2\,m_1(2\,\xi)\,m_0(\xi) \tag{31}$$

$$\vdots$$

$$\hat{\psi}_{L,k}(\xi) \;=\; \hat{\varphi}(\xi)\,\cdot exp(-i\cdot 2^{L+1}k\pi\xi)\cdot\sqrt{2^L}\,m_1(2^{L-1}\xi)\prod_{j=0}^{L-2} m_0(2^j\xi) \tag{32}$$

$$\hat{\varphi}_{L,k}(\xi) \;=\; \hat{\varphi}(\xi)\,\cdot exp(-i\cdot 2^{L+1}k\pi\xi)\cdot\sqrt{2^L}\prod_{j=0}^{L-1} m_0(2^j\xi). \tag{33}$$

Thereby the product in (29)and (32) is taken as 1 in the case $L = 1$. Technical the representation (32) arises from (33) by substituting $m_1(2^{L-1}\xi)$ with $m_0(2^{L-1}\xi)$.

From (28) result with

$$\begin{aligned}
\hat{\varphi}_{1,k}(\xi) &= \sqrt{2}\,\hat{\varphi}(\xi)\cdot exp(-i\cdot 4k\pi\xi)\cdot m_0(\xi) && (34)\\
\hat{\psi}_{1,k}(\xi) &= \sqrt{2}\,\hat{\varphi}(\xi)\cdot exp(-i\cdot 4k\pi\xi)\cdot m_1(\xi) && (35)\\
\hat{\psi}_{2,k}(\xi) &= \sqrt{2}\,\hat{\psi}_{1,k}(2\,\xi) && (36)\\
&\vdots\\
\hat{\psi}_{L,k}(\xi) &= \sqrt{2^{L-1}}\,\hat{\psi}_{1,k}(2^{L-1}\,\xi) && (37)\\
\hat{\varphi}_{L,k}(\xi) &= \sqrt{2^{L-1}}\,\hat{\varphi}_{1,k}(2^{L-1}\,\xi) && (38)
\end{aligned}$$

more simply representations of the above formulas. But the drawback of this simple structured formulas is that $\hat{\varphi}$ must be known and used in a relative great definition domain. So the work with a great array becomes necessary. The functions in (30)-(33) must evaluate only on $[0, 1]$. The dilations of $m_0,\ m_1$ there can be realized simply, because this Fourier-filters are polynomials in $z = -i\cdot 2\,\pi\,\xi$. With (34)-(35) are given the frequency contents to the functions of the first decomposition level. If a deeper decomposition is done then with (37)-(38) are given the corresponding frequency contents of the last level.

For calculation of frequency centers only amplitude spectra are of interest. In this case from (35, (37) and (26) one get the simple equations

$$\begin{aligned}
|\hat{\psi}_{1,k}(\xi)| &= |\hat{\varphi}(\xi)|\cdot\sqrt{2}\,|m_1(\xi)| && (39)\\
|\hat{\psi}_{(1+l),k}(\xi)| &= \sqrt{2}\,|\hat{\psi}_{l,k}(2\xi)| \qquad \text{for} \quad l = 1,\,2,\,\cdots && (40)\\
|\hat{\varphi}_{L,k}(\xi)| &= \sqrt{2^L}\,|\hat{\varphi}(2^L\,\xi)| && (41)
\end{aligned}$$

But if we want to avoid using a great definition array for the approximation of (25) its better to derive from (31)-(33) the equations

$$\begin{aligned}
|\hat{\psi}_{2,k}(\xi)| &= |\hat{\varphi}(\xi)|\cdot 2\,|m_1(2\,\xi)|\,|m_0(\xi)| && (42)\\
&\vdots\\
|\hat{\psi}_{L,k}(\xi)| &= |\hat{\varphi}(\xi)|\cdot\sqrt{2^L}\,|m_1(2^{L-1}\xi)|\prod_{j=0}^{L-2}|m_0(2^j\xi)| && (43)\\
|\hat{\varphi}_{L,k}(\xi)| &= |\hat{\varphi}(\xi)|\cdot\sqrt{2^L}\prod_{j=0}^{L-1}|m_0(2^j\xi)|. && (44)
\end{aligned}$$

and use this for $\xi \in [0,\,1]$. With an appropriate approximation of (25) this formulas provide a good possibility of characterizing the frequency band decomposition of different wavelet systems. The frequency overlappings of neighboring wavelet scales and the sharpness of frequency localization of a chosen scale can be very exactly approximated and visualized. The above remark about the realization of the different dilations to $m_0$ and $m_1$ can be repeated.

The figures 1 - 7 are resulted from this foundation with a corresponding Matlab-program. Based on the normed sampling frequency 1 there the frequency filter behavior of wavelet systems is described. The decompositions begin with first decomposition level $\{\psi_{1,k}(\xi)\}$, the chosen decomposition deepness is 4. Here the logarithmic scaling of the horizontal frequency

axis and the resultant distortions are taken into consideration. In all figures the Nyquist frequency is marked.

As essential examples the following wavelet systems are investigated particularly :

- Daubechies wavelets:
  From figure 1 to 3 the frequency decomposition behavior of the Daubechies wavelets from 'db.1' to db.12 (db.N is a definition in the Wavelet toolbox of Matlab) is shown. One can see how with the increasing length of filters from 2 to 24 the frequency overlapping of neighboring scales is decreasing. Practically beginning with order 5 or 6, where the length of filters is 10 or 12, only directly neighbored Daubechies wavelet scales have common frequency contents.

  In the time domain the Daubechies wavelet 'db.N' of order N has N moments equal to 0. Generally a higher number of vanishing moments is useful for compression purposes, cp [16].

- Symlets:
  In the case of Symlet wavelets which are derived from Daubechies wavelets, and which can be defined as the "least asymmetric" Daubechies wavelets, we have the same situation. Until order 4 they coincide with the Daubechies wavelets. Remark that instability may occur when the order N is too large.

- Coiflets:
  In the time domain Coiflets of order N (coifN in Matlab) are characterized by the following property:

  The wavelet function has 2N moments equal to 0 and the scaling function has 2N-1 moments equal to 0.

  Both functions have now a support of length 6N-1. The functions are much more symmetrical than the Daubechies. The first five filter pairs and first five function pairs (wavelet and scaling function) are implemented in the toolbox, cp [16].

  The figures 4 and 5 illustrate the frequency behavior in the case of decomposition deepness 4. Again with increasing length of filters the frequency overlapping of neighboring scales is decreasing. Practically with order N = 2 or N = 3 beginning, where the length of filters is 12 or 18, only directly neighbored wavelet scales have common frequency contents. This is arrived in the case of Daubechies wavelets with shorter filer lengths, but the approximation properties and the symmetry behavior in time here are much better.

- Biorthogonal spline wavelets:
  In [16] they are constructed on the foundation of B-splines and modified B-splines respectively. Such a B-spline becomes the scaling function $\varphi$ for synthesis and is connected with the reconstruction low-pass filter.
  For analysis (decomposition) and synthesis (reconstruction) you get here different functions, cp. (6) and (7). In time domain one has now full symmetry behavior of the two scaling functions and the two wavelets.
  In [16] such a biorthogonal spline system, which consist in four functions and which is characterized by four filters, is denoted by 'biorN.M'. The implementation is realized for the indices N.M = 1.1, 1.3, ... 4.4, 5.5, 6.8 .
  The figure 6 shows the frequency decomposition behavior of some representatives. It was

developed on the basis of synthesis filters and functions in the system 'biorN.M' , because these functions determine the frequency contents in the FWT.

- Reverse biorthogonal spline wavelets:
  You get them by taking a biorthogonal spline wavelet system and change it's analysis and synthesis filters as well as it's corresponding functions. Now a (modified) B-spline becomes the scaling function $\varphi$ for analysis and is connected with the decomposition low-pass filter.
  In [16] the systems are designed by ReverseBior or 'rbioN.M'. They are implemented also in the cases N.M = 1.1, 1.3, ... 4.4, 5.5, 6.8 .
  Now the figure 7 shows the frequency decomposition behavior of some chosen representatives. It was developed on the basis of synthesis filters and functions in the system 'biorN.M'.

Amongst others this figures show, that upside the Nyquist frequency by FWT the frequencies only partially filtered out. In the cases from db1 to db3 also the second and third decomposition level are influenced clearly yet. From db4 and coif2 on to the end of this classes as well as for bior3.9, bior6.8 and rbio6.8 you can practically assume that only the first level of decomposition is influenced by frequencies upside the Nyquist frequency. This means that by using here only levels of FWT higher than 1 in signal analysis it becomes not necessary to apply additional filters. So one can suggest to use a sample frequency which at least for times greater than the highest dominating frequency of the researched system.

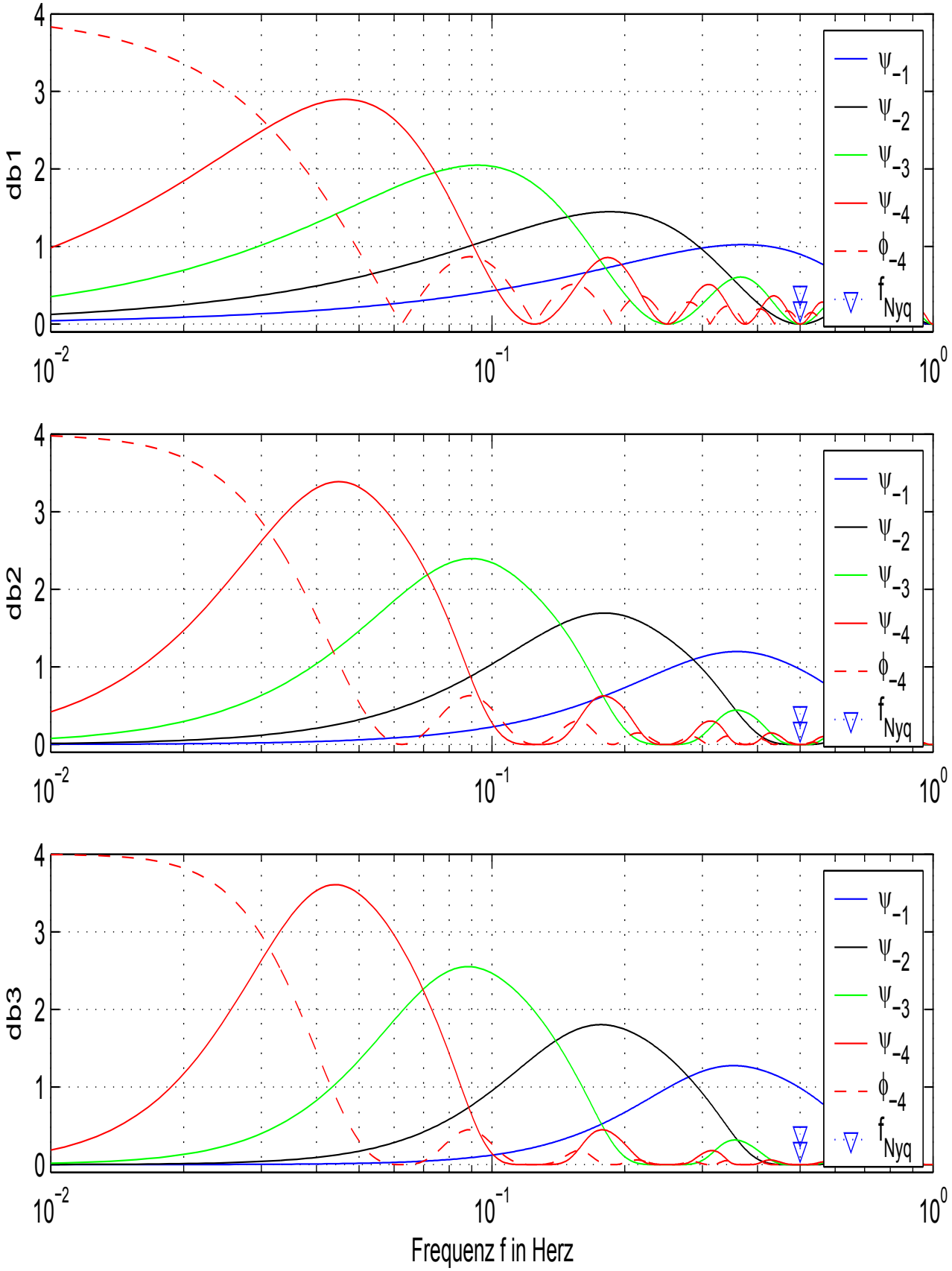


Figure 1: Amplitude spectra of Daubechies-wavelets

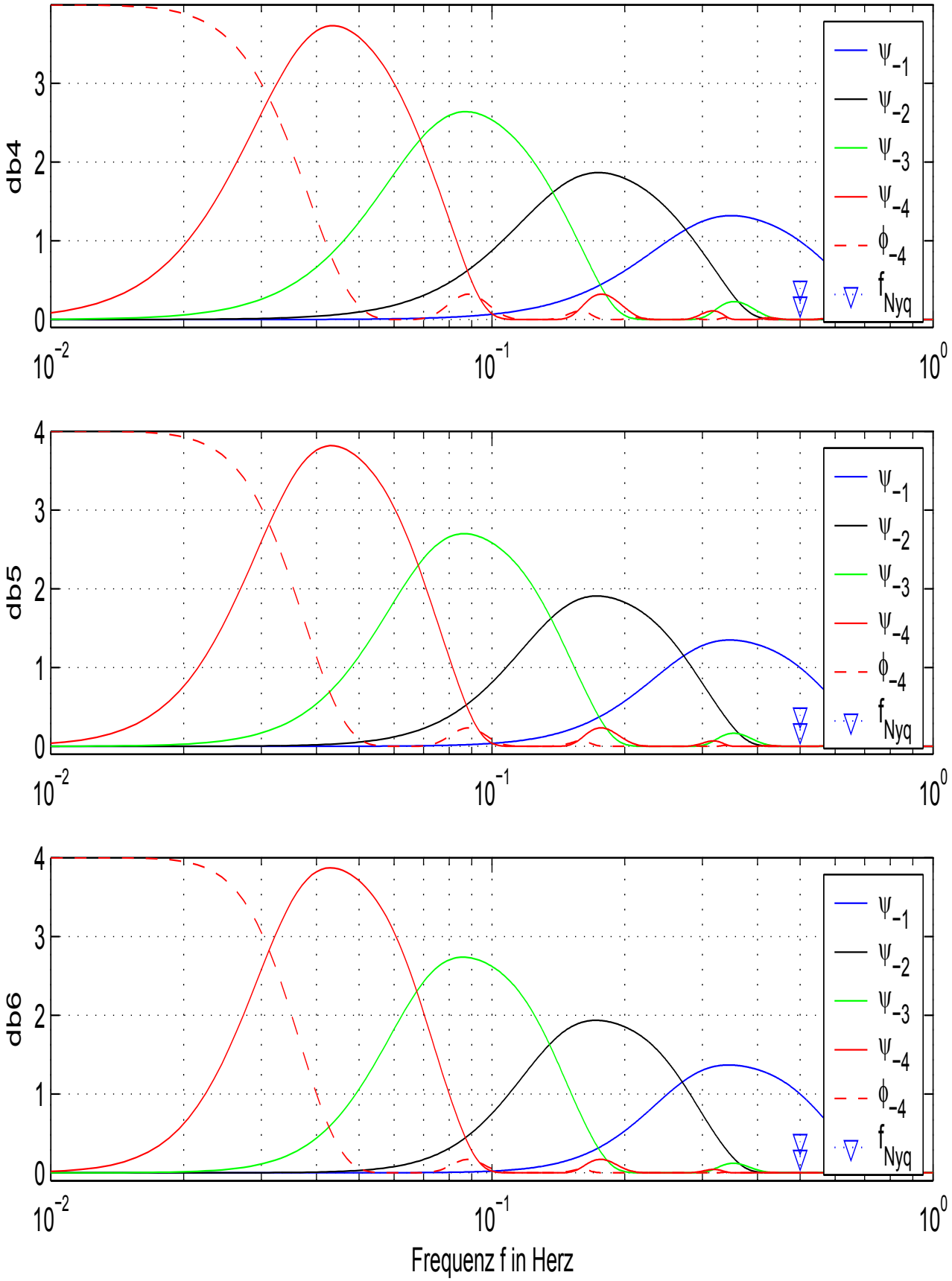


Figure 2: Amplitude spectra of Daubechies-wavelets

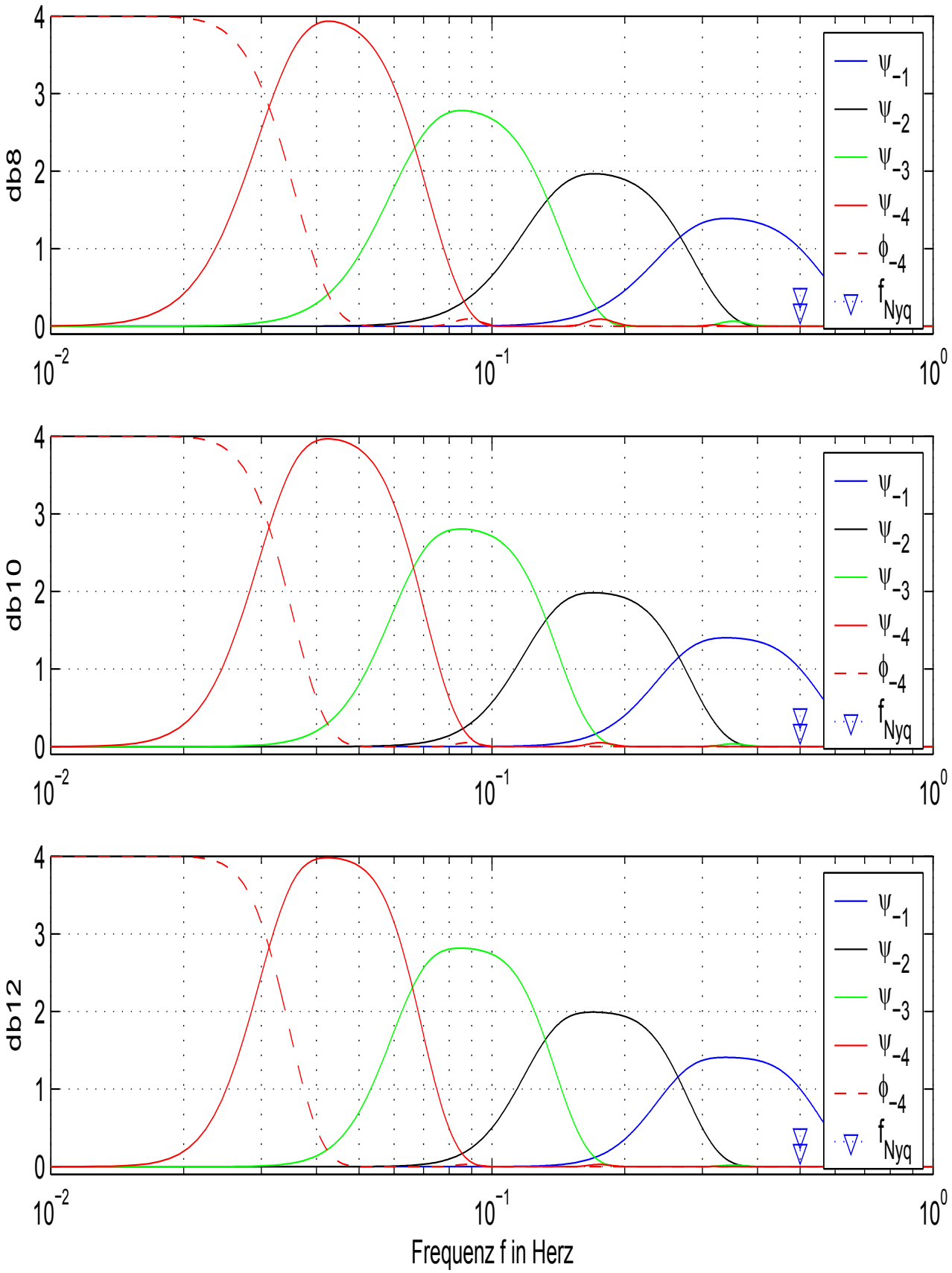


Figure 3: Amplitude spectra of Daubechies-wavelets

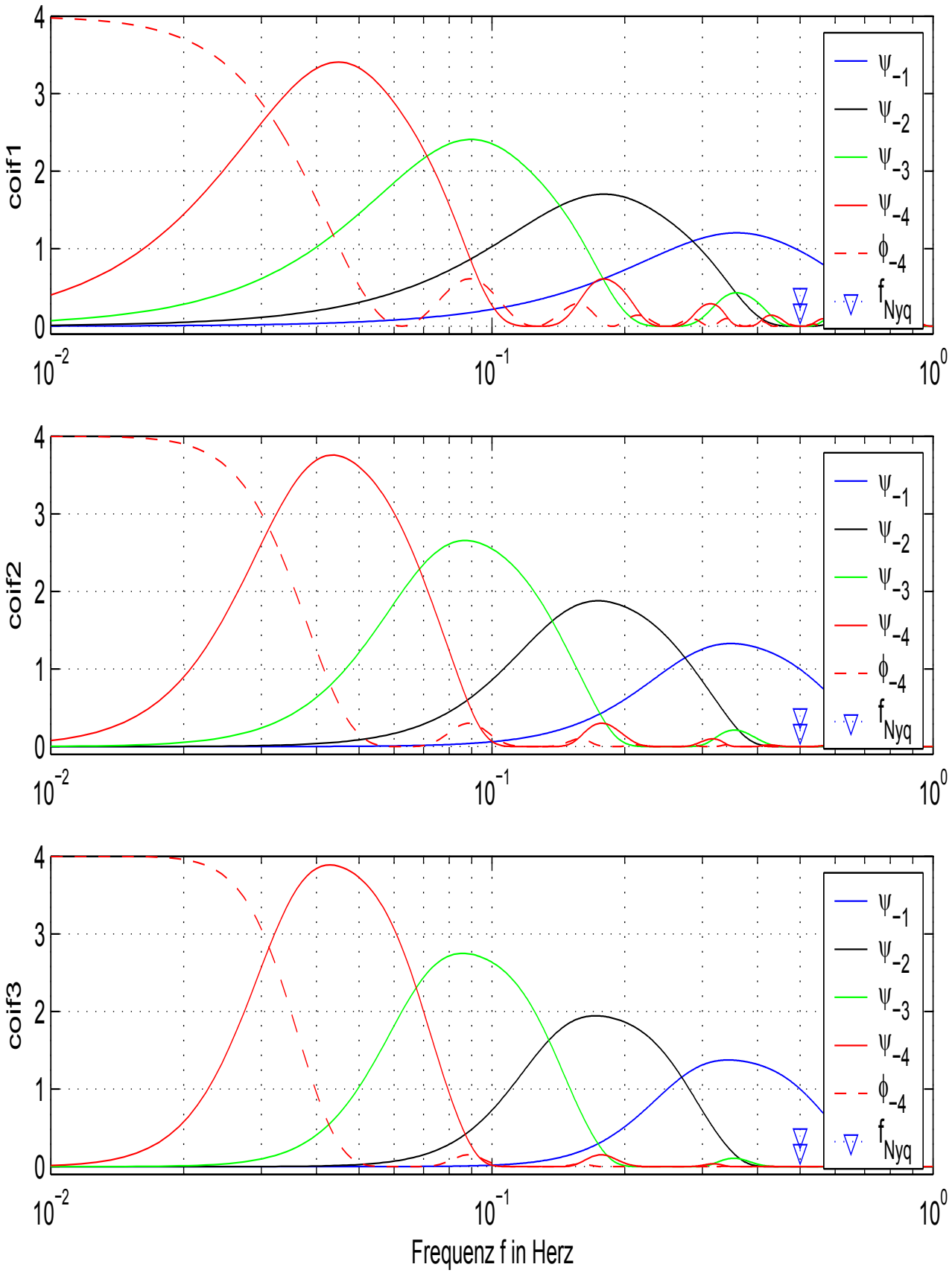


Figure 4: Amplitude spectra of Coifman-Funktionen

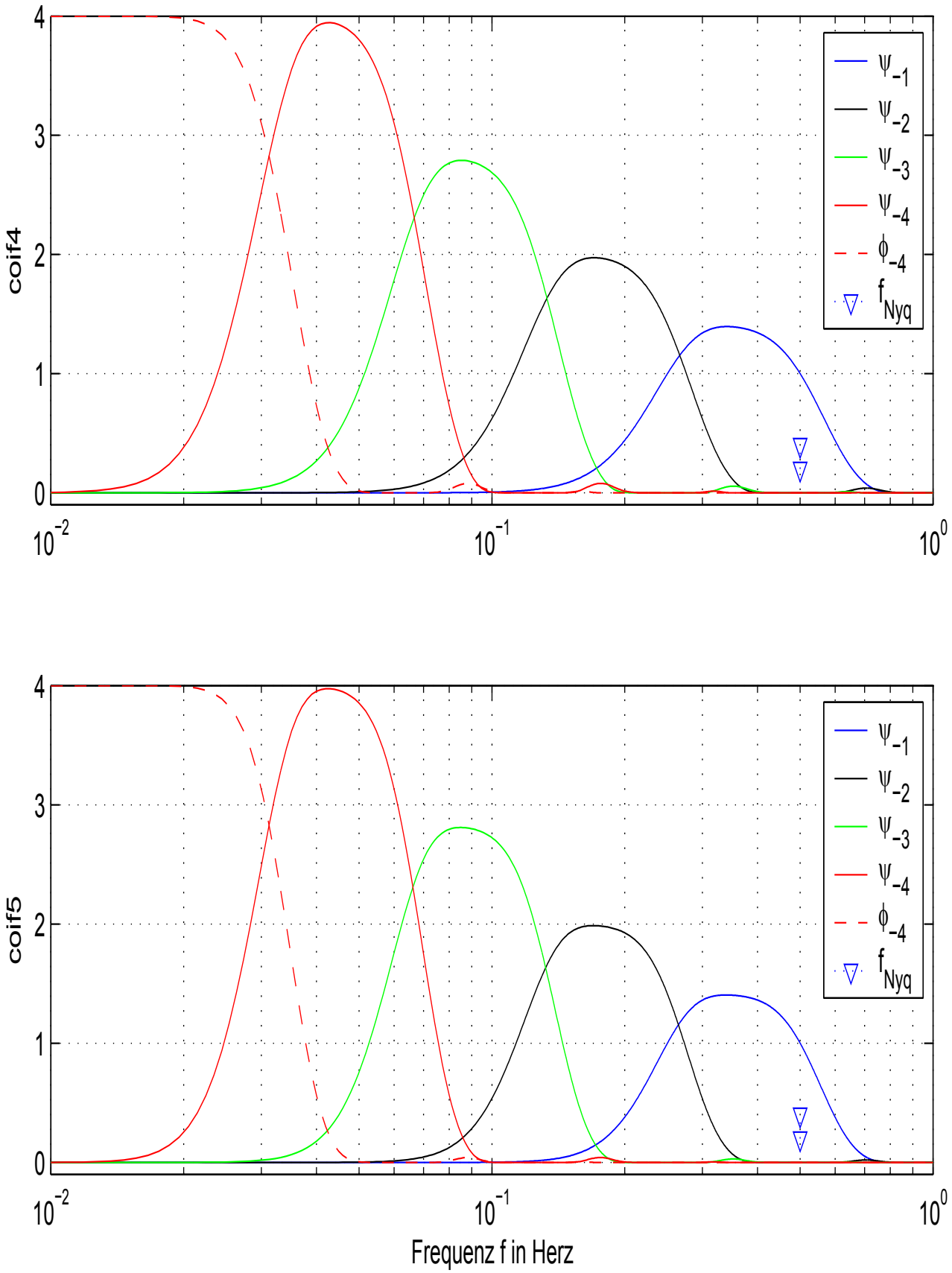


Figure 5: Amplitude spectra of Coifman-Funktionen

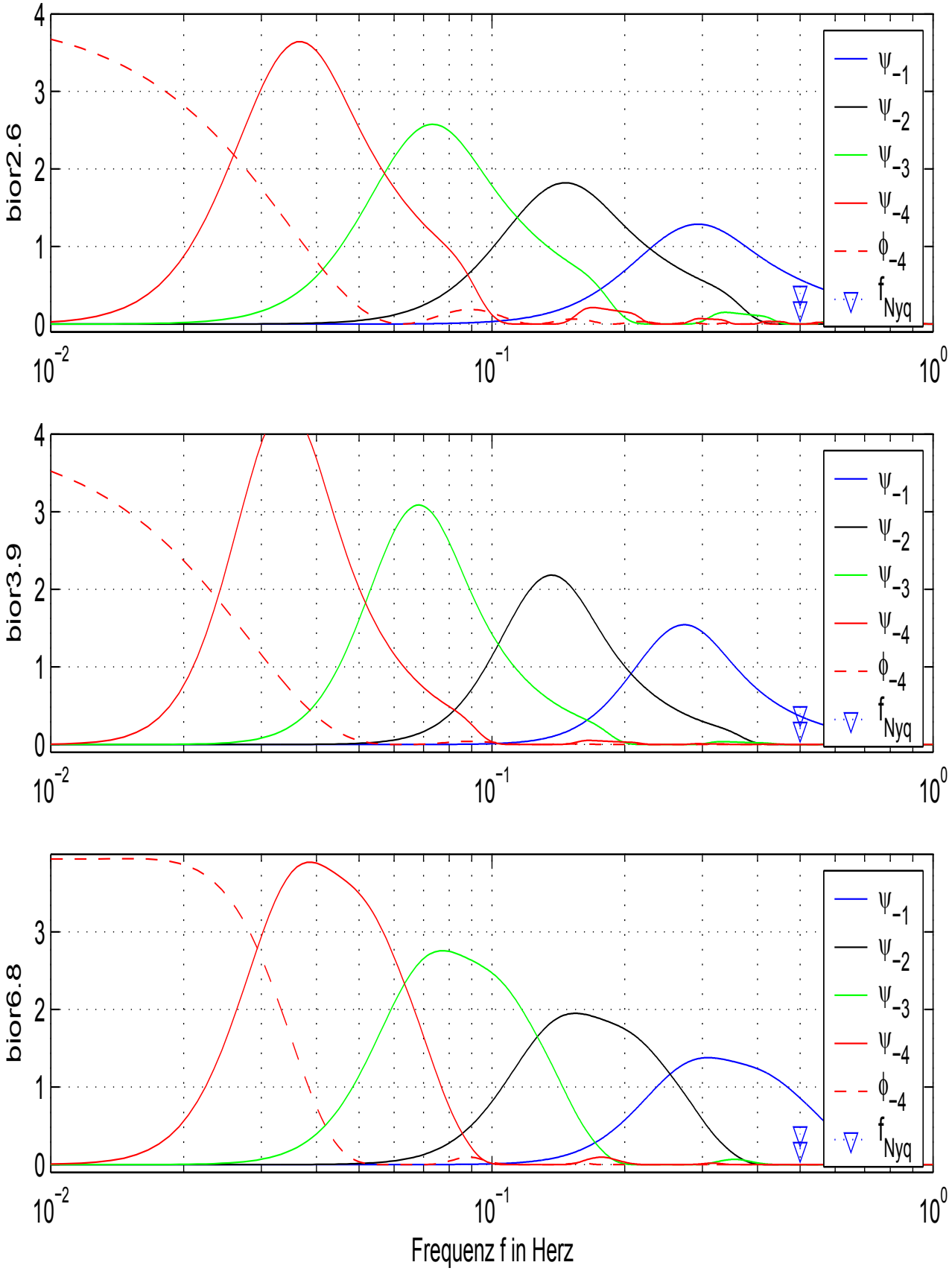


Figure 6: Amplitude spectra of synthesis wavelets of biorN.M

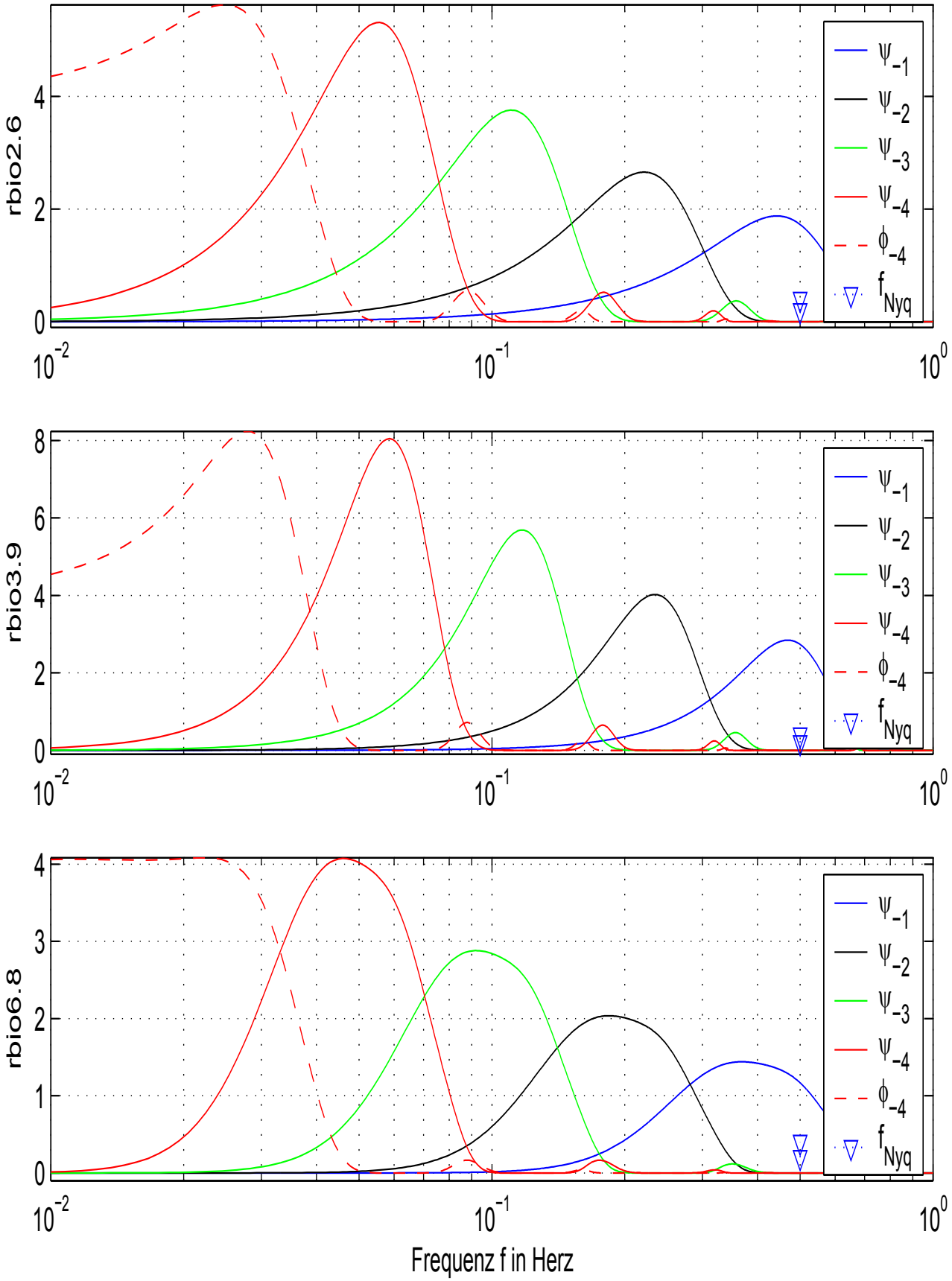


Figure 7: Amplitude spectra of synthesis wavelets of rbioN.M

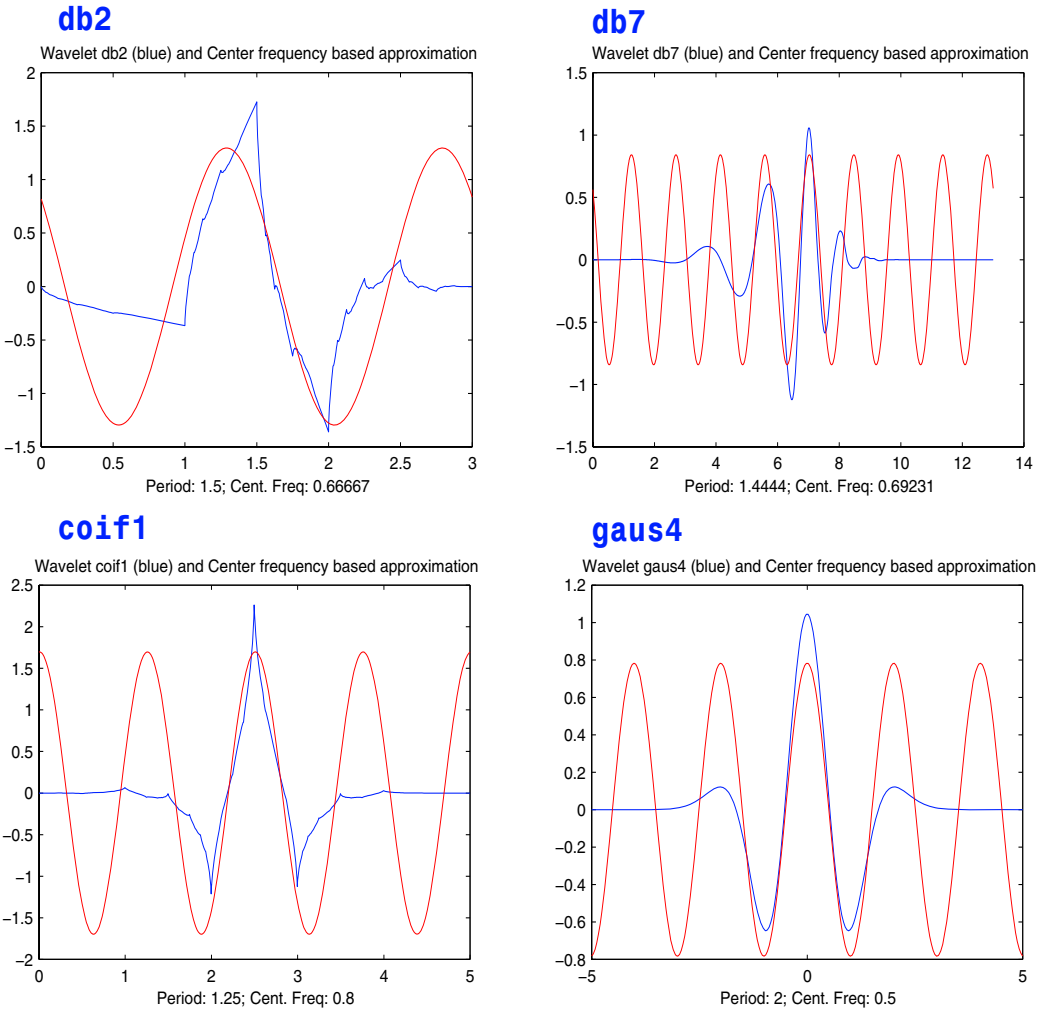


Figure 8: Center Frequencies for some Wavelets

## 4 FREQUENCY CENTERS OF THE WAVELET BANDS

In [16], p. 6-68 the relationship between scale and frequency is considered. The notion frequency is a little broad and it would be more correctly to speak about the frequency center corresponding to a chosen scale of the wavelet decomposition. Also the notion pseudo-frequency of a wavelet scale is used in this context.

The figure 8 shows some examples generated using the frequency center approximation of cp. [16]. Here are Daubechies wavelets of order 2 and 7, the coiflet of order 1, and the Gaussian derivative of order 4 are chosen. The last wavelet has no scaling function and there exist no discrete filters h and g. This means, that formula (25) can't used in this case.

The above center frequency-based approximations comprehend the main wavelet oscillations. The frequency center is a convenient and simple characterization of the leading dominant frequency of a given wavelet.

By [16] for a mother wavelet (basic wavelet) the center of frequency is computed applying the Fast Fourier Transform (FFT) to an approximated time representation. This time domain approximation is obtained with the help of the so called cascade algorithm, which there will be

| db1 | db2 | db3 | db4 | db5 | db6 | db7 | db8 | db9 |
|---|---|---|---|---|---|---|---|---|
| 0.371 | 0.359 | 0.354 | 0.35 | 0.346 | 0.344 | 0.342 | 0.342 | 0.34 |
| | | | sym4 | sym5 | sym6 | sym7 | sym8 | sym9 |
| | | | 0.35 | 0.346 | 0.344 | 0.342 | 0.342 | 0.34 |
| coif1 | coif2 | coif3 | coif4 | coif5 | | | | |
| 0.359 | 0.348 | 0.344 | 0.342 | 0.34 | | | | |
| bior2.6 | rbio2.6 | bior3.9 | rbio3.9 | bior6.8 | rbio6.8 | | | |
| 0.443 | 0.293 | 0.469 | 0.273 | 0.369 | 0.309 | | | |

Table 1: Frequency center $\xi_1$ to the decomposition level produced with product formula

| db1 | db2 | db3 | db4 | db5 | db6 | db7 | db8 | db9 |
|---|---|---|---|---|---|---|---|---|
| 0.498 | 0.333 | 0.400 | 0.357 | 0.333 | 0.364 | 0.346 | 0.333 | 0.353 |
| | | | sym4 | sym5 | sym6 | sym7 | sym8 | sym9 |
| | | | 0.357 | 0.333 | 0.364 | 0.346 | 0.333 | 0.353 |
| coif1 | coif2 | coif3 | coif4 | coif5 | | | | |
| 0.4000 | 0.3636 | 0.3529 | 0.3478 | 0.3448 | | | | |
| bior2.6 | rbio2.6 | bior3.9 | rbio3.9 | bior6.8 | rbio6.8 | | | |
| 0.4617 | 0.3078 | 0.4738 | 0.2632 | 0.3824 | 0.3236 | | | |

Table 2: Frequency center $\xi_1$ to the first decomposition level produced with Matlab-wavefun

realized by

$$[phi, psi, xval] = wavefun(wavelet, N). \tag{45}$$

The procedure wavefun in [16] uses the single-level inverse wavelet transform repeatedly N times to approximate the scaling function on a grid of $2^N$ points. The corresponding array of the basic wavelet arises then from (6) with the decomposition synthesis filter $g$.

This procedure is possible because for the scaling function one has $\varphi = \varphi_{0,0}$ and this corresponds to $P_0(\varphi) = \varphi$ with interval and all other $\tilde{S}_{0,k}$ zero in (17). So (45) realizes the array of $\varphi$ with N steps of (21), whereby all $\tilde{W}_{\nu,r} = 0$ and at the starting level only $\tilde{S}_{0,0} = 1$ is to regard. On a grid of length $2^N$ the approximation values then are given by the $\tilde{S}_{N,k}$. This all is done in [16] by the procedure centfrq. The procedure scal2frq computes then the frequency center of every implemented wavelet by taking into account the scale a and the sampling period $\Delta$, cp. (48).

Contrary to the above treatment of [16], where first a piecewise linear approximation of the wavelet with iterations of the cascade algorithm is produced followed by FFT and frequency maximizing the modulus, here an other procedure is developed. This procedure works in the case of orthogonal and biorthogonal Wavelet systems, for which scaling functions and wavelets are defined over discrete filters. It uses the representation (39) with an appropriate approximation of (25) in the interval $[0,\ 1]$. Now the dominated frequency $\xi_1$ like in the other method can be found as the value, which maximizes the modulus (39). Note that with $\xi_1$ the frequency center of the first decomposition level is given, assumed sampling rate is 1 (normed case). If you compare the results with [16] you must note that

$$\xi_0 = 2\,\xi_1 \qquad \text{for the center of the basic wavelet} \quad \psi = \psi_{0,0} \tag{46}$$

which is of level 0. The entries in the tables 1 and 2 are done for the level 1, this means that there are compared the centers $\xi_1$ calculated by the different methods. If one accept this associated

| | | | | | | | | |
|---|---|---|---|---|---|---|---|---|
| db1<br>0.297 | db2<br>0.286 | db3<br>0.279 | db4<br>0.275 | db5<br>0.272 | db6<br>0.270 | db7<br>0.269 | db8<br>0.268 | db9<br>0.267 |
| | | | sym4<br>0.275 | sym5<br>0.272 | sym6<br>0.270 | sym7<br>0.269 | sym8<br>0.268 | sym9<br>0.267 |
| coif1<br>0.2852 | coif2<br>0.2739 | coif3<br>0.2695 | coif4<br>0.2666 | coif5<br>0.2646 | | | | |
| bior2.6<br>0.3032 | rbio2.6<br>0.2280 | bior3.9<br>0.3125 | rbio3.9<br>0.2065 | bior6.8<br>0.2817 | rbio6.8<br>0.2534 | | | |

Table 3: $\xi_{tp}(1)$ - Frequency predominance transition point between 1. and 2. level

frequency $\xi_1$, then with $\xi_\nu(\psi)$ for the variants of the $\nu$-th wavelet decomposition level and with $\xi_\nu(\psi, \Delta)$ taking into consideration an underlying sampling period $\Delta$

$$\xi_\nu(\psi) = \xi_0(\psi_{\nu,k}) = \frac{\xi_0(\psi)}{2^\nu} \qquad \text{and} \qquad \xi_\nu(\psi, \Delta) = \frac{\xi_0(\psi)}{\Delta \cdot 2^\nu} \tag{47}$$

result. For (a,b)-variants which not always connected with the decomposition tree one has

$$\frac{1}{\sqrt{a}}\,\psi\left(\frac{t-b}{a}\right) \quad \longmapsto \quad \frac{\xi_0}{a} \tag{48}$$

On the $\nu$-th decomposition level of the FFT is $a = 2^\nu$.

In the figures 1 to 7 you can recognize the transition points for frequency predominance for neighbored decomposition levels. The points of transition between the 1. and 2. level are calculated here with the help of product formula. They are noted by

$$\xi_{tp}(1) = \xi_{tp}(\psi, 1) \qquad \text{- transition point between 1. and 2. level} \tag{49}$$

and shown in table 3. Between the 0. and 1. level you get

$$\xi_{tp}(0) = \xi_{tp}(\psi, 0) = 2 \cdot \xi_{tp}(\psi, 1) \tag{50}$$

which is not important for FWT-decomposition but gives with

$$\xi_{tp}(\nu) = \xi_{tp}(\psi, \nu) = \frac{\xi_{tp}(\psi, 0)}{2^\nu} \tag{51}$$

a simpler formula for the consecutive transition points between the $\nu$-th and $(\nu+1)$-th level. Assuming an first asymmetric bulk of $|\hat{\psi}_{1,k}|$ one could think it's better to calculate the associated frequency center of the first decomposition level by one of the following formulas

$$\xi^p(\psi, 1) = \frac{\int_0^{0.5} \xi \cdot |\hat{\psi}_{1,k}(\xi)|^p d\xi}{\int_0^{0.5} |\hat{\psi}_{1,k}(\xi)|^p d\xi} \qquad \text{for} \quad p = 1,\, 2,\, \cdots \tag{52}$$

but the considerations of the next paragraph seem this to suggest not.

At last a measure for frequency overlapping of the first and second scale can be calculated by

$$overlap_{1,2} = \frac{\int_0^1 |\hat{\psi}_{1,0}(\xi)| \cdot |\hat{\psi}_{2,0}(\xi)| d\xi}{\sqrt{\int_0^1 |\hat{\psi}_{1,0}(\xi)|^2 d\xi \cdot \int_0^1 |\hat{\psi}_{2,0}(\xi)|^2 d\xi}} \tag{53}$$

$$= \frac{\int_0^1 |\hat{\psi}_{1,0}(\xi)| \cdot |\hat{\psi}_{1,0}(2\xi)| d\xi}{\sqrt{\int_0^1 |\hat{\psi}_{1,0}(\xi)|^2 d\xi \cdot \int_0^1 |\hat{\psi}_{1,0}(2\xi)|^2 d\xi}} \tag{54}$$

in a practical sense. If you define frequency overlapping of the $j$-th and $(j+1)$-th scale analogous by

$$overlap_{j,j+1} = \frac{\int_0^{K(j)} |\hat{\psi}_{j,0}(\xi)| \cdot |\hat{\psi}_{j,0}(2\xi)| d\xi}{\sqrt{\int_0^{K(j)} |\hat{\psi}_{j,0}(\xi)|^2 d\xi \cdot \int_0^{K(j)} |\hat{\psi}_{j,0}(2\xi)|^2 d\xi}} \tag{55}$$

then by choosing $K(j) = 2^{1-j}$ you get exactly

$$overlap_{1,2} = overlap_{j,j+1} \qquad \text{for all} \quad j \in \mathbb{Z}. \tag{56}$$

By this formula only the first bulk of the corresponding $|\hat{\psi}_{j,0}|$ has been borne in mind. If you set $K(j) = 2^{1-j}$ in (55) then you get an increasing sequence $overlap_{j,j+1}$, which can also be described substituting all upper integration limits in (53) by $2^{j-1}$. If this sequence increases slowly, which would better proofed with (42)-(43), the simple formulas (56) can be taken.

The above considerations can be carried forward to the case of Wavelet Packet Transform where more frequency bands are produced. There to every node exist one frequency band. Especially the higher bands produced by FWT which are also broader can successive divided in different smaller ones.

## 5 THE FWT OF PURE OSCILLATIONS

In the case of an orthogonal wavelet you can verify the above results also by interpretation the Continuous Wavelet Transform (CWT) in its frequency representation

$$CWT(f,a,b) = \frac{1}{\sqrt{a}} \int_{-\infty}^{\infty} f(t)\, \psi\left(\frac{t-b}{a}\right) dt \tag{57}$$

$$= \sqrt{a} \int_{-\infty}^{\infty} \overline{\hat{f}(\xi)}\, \hat{\psi}\,(a\xi)\; e^{-ib2\pi\xi} d\xi. \tag{58}$$

Now in particular for orthogonal wavelets the decomposition coefficients of (18) and (19) are determined by

$$\tilde{W}_{j,k} = W_{j,k} = CWT(f, 2^j, k \cdot 2^j), \qquad j = 1, 2, \cdots, L\,. \tag{59}$$

For a biorthogonal wavelet system corresponding to the here made notation you must substitute in (57)-(58) the wavelet $\psi$ by $\tilde{\psi}$ and the corresponding Fourier-transform $\hat{\psi}$ by $\hat{\tilde{\psi}} = \mathcal{F}(\tilde{\psi})$ to get the coefficients $\tilde{W}_{j,k}$ of the FWT-analysis (18) and (19) with the integral transformation (59).

To simplify matters in the next example let from now on the Fourier-transform of $\tilde{\psi}$ be noted as $\hat{\psi}$. With $\hat{\psi} := \mathcal{F}(\tilde{\psi})$ let's now use (58) to describe the principle behavior of the FWT $\{\tilde{W}_{j,k}\}$ when applied on harmonic functions. The Fourier-transform of

$$f(t) = cos(2\pi\xi^* t + \alpha) \tag{60}$$

is

$$\hat{f}(\xi) = \frac{1}{2}\, e^{i\alpha}\, \delta\,(-\xi + \xi^*) + \frac{1}{2}\, e^{-i\alpha}\, \delta\,(\xi + \xi^*)\,. \tag{61}$$

Apply (58) and get

$$CWT(f, a, b) = \frac{1}{2}\sqrt{a}\, \left(e^{-i\alpha}\, \hat{\psi}\,(a\,\xi^*)\; e^{-i2\pi\xi^* b} + e^{i\alpha}\, \hat{\psi}\,(-a\,\xi^*)\; e^{i2\pi\xi^* b}\right). \tag{62}$$

In the case of a real valued wavelet $\tilde{\psi}$ this transform can be written as

$$CWT(f, a, b) = \sqrt{a}\, \Re\left(\hat{\psi}\,(a\,\xi^*)\; e^{-i(2\pi\xi^* b + \alpha)}\right) \tag{63}$$

with $\Re(\hat{\psi})$ as the real part of $\hat{\psi}$. So you get over

$$CWT(f, a, b) = \sqrt{a}\, \left|\hat{\psi}\,(a\,\xi^*)\right| \cos\left(2\,\pi\,\xi^*\, b + \alpha - \arg(\hat{\psi}(\xi^*\, a))\right) \tag{64}$$

the coefficients of the FWT

$$\begin{aligned} \tilde{W}j,k &= \sqrt{2^j}\, \left|\hat{\psi}\left(2^j\xi^*\right)\right| \cos\left(2^{j+1}\,\pi\,\xi^*\, k + \alpha - \arg(\hat{\psi}(2^j\xi^*))\right) \\ &= |\hat{\psi}_j(\xi^*)|\, \cos\left(2\pi\,\xi^*\,\{2^j\, k\} + \alpha - \arg(\hat{\psi}(2^j\xi^*))\right). \end{aligned} \tag{65}$$

This formulas are valid for every practical used analysing wavelet with compact support in time. For this wavelets the conclusion

$$\tilde{\psi} \in L_0^2\,(\mathbb{R}) \cap L_0^1\,(\mathbb{R}) \quad \Longrightarrow \quad \hat{\psi} \in C^k(\mathbb{R}) \quad \forall k \in \mathbb{N}$$

is valid. The formula (65) is not difficult to deduce, but I didn't find it anywhere. In the context of analysing time-frequency behavior of signals with FWT the formula (65) becomes very useful. Looking at (60) and it's FWT (65) you can conclude that an oscillation with frequency $\xi^*$ provides in the range of FWT on every decomposition scale an oscillation with calculable shifting and frequency $2^j \cdot \xi^*$ if whole-numbered sampling $\{k\}$ is assumed. In the wavelet-toolbox of Matlab as generally with growing index scaling $j$ (here connected with sinking frequency) is growing dyadic sampling in the time-scale realized. This means that the sampling rate grows up with factor 2 scale by scale and becomes $2^j$ on scale j. So on every vertical line characterized by constant $k$ the FWT-values in all present nodes only differ by the factors $|\hat{\psi}_j(\xi^*)|$ in (65).

## REFERENCES


[1] G. Beylkin & B. Torresani, *Implementation of Operators via Filter Banks.* Applied and Computational Harmonic Analysis 3, 1996, 164–185.

[2] M. Brehm, K. Markwardt and V. Zabel, *Applications of Wavelet Packets in System Identification.* Jahrestagung der GAMM, 2005, Université du Luxembourg.

[3] M. Brehm, K. Markwardt and V. Zabel, *Applications of Biorthogonal Wavelets in System Identification.*, Proceedings of the European Congress on Computational Methods in Applied Sciences and Engineering (ECCOMAS 2004), Jyväskyla, Neittaanmäki, Rossi, K. Majava& O.Pironneau (eds.).

[4] I. Daubechies, Time-Frequency Localisation Operators : A Geometric Phase Space Approach, IEEE Trans. Inform. Theory, Vol. 34(4), 1988, pp. 605-612

[5] I. Daubechies, Orthonormal Bases of compactly supportet Wavelets, Comm. Pure Appl. Math., Vol. 41(7), 1988, pp. 909-996

[6] I. Daubechies, Orthonormal Bases of compactly supportet Wavelets II. Variations on the Theme, SIAM J. Math. Anal., Vol. 24(2), 1993, pp. 499-519

[7] A. Cohen, I. Daubechies & J.C. Feauveau, *Biorthogonal bases of compactly supported wavelets.* Communications on Pure and Applied Mathematics, IEEE Transactions on Signal Processing, Vol.XLV, 485–560, 1992.

[8] A. Cohen, *Biorthogonal Wavelets.* Wavelets in Analysis and Applications II, 123–152, Academic Press 1992.

[9] W.M. Lawton, *Necessary and sufficient conditions for constructing orthonormal wavelet bases.* J. Math. Phys.32(1), 1440–1443, 1991.

[10] K. Markwardt, *Application of Fast Wavelet Transformation in Parametric System Identification*, selected to be published 2006 in the volume Wavelet Analysis and Applications of the Springer (SCI) book series Applied and Numerical Harmonic Analysis

[11] K. Markwardt, *Application of Fast Wavelet Transformation in Parametric System Identification*, 4th International Conference on Wavelet Analysis and Its Applications, University of Macau, China, 30th November - 2nd December, 2005

[12] K. Markwardt, *Die schnelle Wavelet-Transformation als Grundlage für Verfahren zur System- und Parameteridentifikation.* Manuscript, pages 1–125 (2005), not published yet.

[13] K. Markwardt, *Biorthogonale Wavelet-Systeme in der Parameteridentifikation.* Proceedings of the 16th IKM 2003, Gürlebeck, Hempel & Könke (eds.), Weimar, Germany, June 10-12, 2003.

[14] K. Markwardt, *Systemanalyse und Parameteridentifikation mit Hilfe der schnellen Wavelet-Transformation.* Forschungbericht, 1–76, 2002, ISM, BUW, Weimar.

[15] K. Markwardt, *Betrachtungen zur Anwendung der Wavelet-Transformation in der Systemidentifikation.* 6. Institutskolloquium des ISM der BUW, Bericht 1/00, 2000, 107–126, Bucher, Burkhardt & Vormwald (eds.).

[16] M. Misiti, Y. Misiti, G.Oppenheim and J.-M. Poggi, Wavelet Toolbox for Use with MATLAB, March 2006, Wavelet Toolbox Users Guide, COPYRIGHT 19972006 by The MathWorks, Inc.

[17] Resnikoff, *Wavelet Analysis.* Springer, 1998

[18] M. V. Wickerhauser, Lectures on Wavelet Packet Algorithms, Washington University, St. Louis, Missouri, 1991

[19] V. Zabel, *Applications of Wavelet Analysis in System Identification.* Dissertation, 2003, Institute Structural Mechanics, Faculty of Civil Engeneering, Bauhaus-University Weimar